JOURNAL OF THEORETICAL
AND APPLIED MECHANICS
41, 2, pp. 215-240, Warsaw 2003

ANALYSIS OF PARAMETRIC MODELS OF MR LINEAR DAMPER

Bogdan Sapiński
Jacek Filuś

Department of Process Control, University of Mining and Metallurgy
e-mail: deep@uci.agh.edu.pl

This work deals with the analysis of parametric models of a MR linear damper, which suit various rheological structures of the MR fluid. The MR fluid structure and properties, damper description and parametric damper models which are connected in various ways with the actual behaviour of the MR fluid are presented. Based on computer simulations, the effectiveness of the models under predicted MR linear damper behaviour is shown. The values of the parametric models used in the simulations were determined in an identification experiment.

Key words: MR fluid, MR damper, rheological structure, modelling, identification, simulation

1. Introduction

MR dampers draw attention not only from a phenomenological point of view, but also from hope associated with their practical application in vibration control of a dynamic structure. From the phenomenological viewpoint, the most important factors are, above all, high non-linear characteristics of these dampers (Gandhi and Chopra, 1996; Kamath and Werely, 1997; Snyder *et al.*, 2000; Stanway *et al.*, 2000; Wereley *et al.*, 1998). Accordingly, a hysteresis and jump-type phenomenon appears, which characterises the behaviour of MR fluids. The explanation for these appearances depends on velocity. The relationship between the damping force and piston velocity for a linear MR damper of low efficiency is illustrated in Fig. 1. This means that the non-linearity of hysteresis has greater significance for lower velocities, while for higher velocities non-linear jumps dominate.

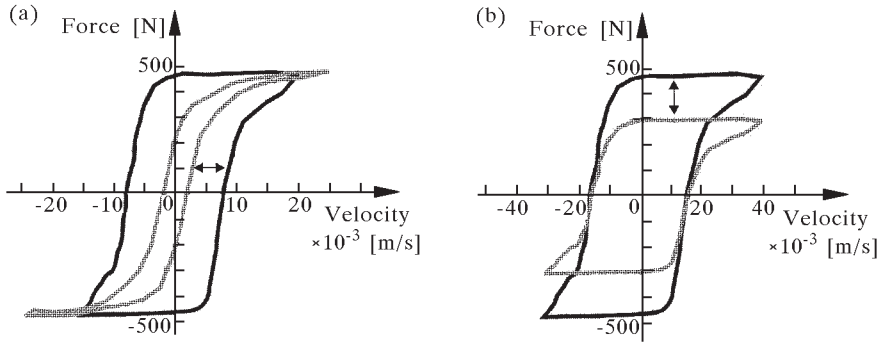

Fig. 1. Character of force-velocity curve at: (a) low velocities – hysteresis phenomenon, (b) higher velocities – jump-type phenomenon

These non-linearities create difficulties in the acceptance of such phenomenological MR damper models, which make the behavioural prediction in its whole operating range impossible. They can also create limitations in the practical application of MR dampers. However, MR dampers contain certain features such as, quick response to changes of the control signal, full reflexivity of MR fluid transformations and low power consumption. These create the assumption that, in the future, MR dampers will be applied successfully to semi-active vibration control systems. Examples of the commercial use of MR dampers have already been presented in, among others, Carlson and Sproston (2000).

In the modelling, MR dampers can be divided into two main methods, parametric and non-parametric. In the parametric method, the damper is characterised by a system of linear and non-linear elements, which define the parameters of springs, dashpots and other mechanical elements, controlling the mechanisms and their operating area (Dyke *et al.*, 1996). In the non-parametric method, the damper is characterised by special well- suited functions (such as polynomials, hyperbolic tangent, delay, offset), or by a polynomial with the power of damper piston velocity (Choi *et al.*, 2001), and the artificial intelligence methods (fuzzy logic or neural networks) (Sapiński, 2002).

In this paper, the description of parametric models of a MR linear damper closely associating the actual MR fluid behaviour (Table 1) have been analytically formulated based on rheological laws. In these models, the damper is treated as a stationary system, whose dynamics can be described by differential equations.

Table 1. Phenomenological parametric models of MR dampers considering various rheological MR fluid behavioural scenarios

No.	MR damper model	MR fluid rheological behaviour			
		viscotic	elastic	plastic	histeresis
1	Bingham	✓		✓	
2	Bingham body	✓	✓	✓	
3	Gamota-Filisko	✓	✓	✓	
4	Li	✓	✓	✓	
5	Bouc-Wen	✓	✓		✓
6	Spencer	✓	✓		✓

The acceptance of various rheological structures for the characterisation of MR fluid properties shows the effectiveness associated with these models as tools for prediction of the actual damper behaviour. Necessary for this is the knowledge of parametric values of the model, which are designated on the basis of experiments undertaken for different periodic kinematic excitations of the piston and at several levels of the control current in the damper coil (Sapiński, 2002).

2. Structure and properties of MR fluids

MR fluids belong to a group of fluids which are non-Newtonian, rheologically stable, with a shear yield strength, and are controlled by a magnetic field. These fluids are non-coloidal suspensions with magnetic particles of high concentration in a non-magnetic fluid carrier. The materials applied as the magnetic particles are soft magnetic compounds (most common ferrous oxide Fe_2O_3 and Fe_3O_4 with magnetic saturation of about 1.9 T). Water, silicon, mineral or synthetic oil and glycerol act as fluid carriers. Magnetic particles have a diameter of between 0.5 μm and 8 μm, therefore the MR fluids are also known as microfluids, as opposed to nanofluids and ferrofluids (Bolter and Janocha, 1998).

The rheological properties of MR fluids depend on the concentration of magnetic particles, their size, shape, properties of fluid carriers, magnetic field intensity, temperature and also other factors (Jolly *et al.*, 1999; Weiss *et al.*, 1994). The interrelation of these factors is complex. The most important parameters of MR fluids are; maximum shear yield stress $(50 \div 100)$ kPa, maximum magnetic field $\cong 250$ kA/m, plastic viscosity $(0.1 \div 1.0)$ Pa·s, operating

temperature $(-50 \div 150)$°C, density $(3 \div 4)\,\mathrm{g/cm^3}$. An essential feature of a MR fluid is its insensitivity to contamination. When no separate external magnetic field is applied ($H = 0$), the concentration of particles is diffused in the fluid carrier (Fig. 2a), their magnetic moments are randomly directed and resultantly attain the zero value. The MR fluid shows then Newtonian behaviour.

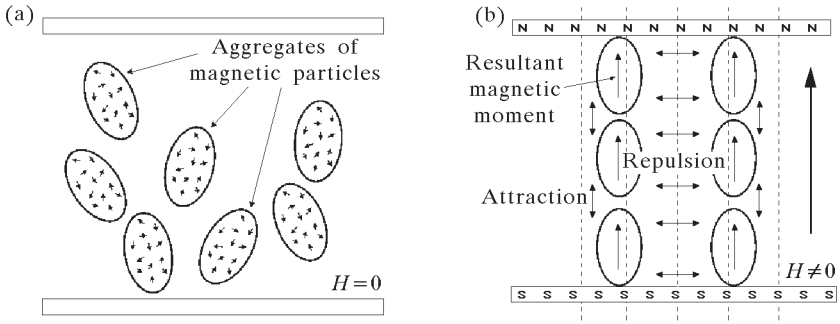

Fig. 2. Behaviour of MR fluid: (a) $H = 0$, (b) $H \neq 0$

In a magnetic field ($H \neq 0$), the aggregates are polarised and their magnetic moments occur along the field lines in the MR fluid. These aggregates create chain-like structures which run parallel to the field lines (Fig. 2b) and do not show thermal movements. The energy of the mechanisms necessary to create the chain structures increases alongside any increase in the magnetic field. These MR fluid properties change as a result of a meaningful formation of the shear stress, which in turn creates an increase in the viscosity.

In their rheological behaviour, MR fluids can be divided into two characteristic areas, pre- and post yield (Li *et al.*, 2000), to which the characteristic shear stresses $\tau_{y,d}$ and $\tau_{y,s}$ are respectively connected (Fig. 3). The values of $\tau_{y,d}$ and $\tau_{y,s}$ respectively mean that; dynamic shear yield stress (Ginder, 1996) (defined as the point of the zero-rate of the linear regression curve fit) and the static shear yield stress (defined as the shear stress necessary to initiate MR fluid flow) depend on the magnetic field.

In the pre-yield area the MR fluid shows visco-elastic properties and a part of the energy required is regained (elastic behaviour) and a part is dissipated in the form of heat (viscotic behaviour). This behaviour can be explained by the linear visco-elastic theory.

The Bingham body model is often applied in the research of MR fluid behaviour. In this model, in the post-yield area (for a stress greater than the shear stress, which depends on the magnetic field strain H, i.e. for $\tau \geqslant \tau_{y,d}$)

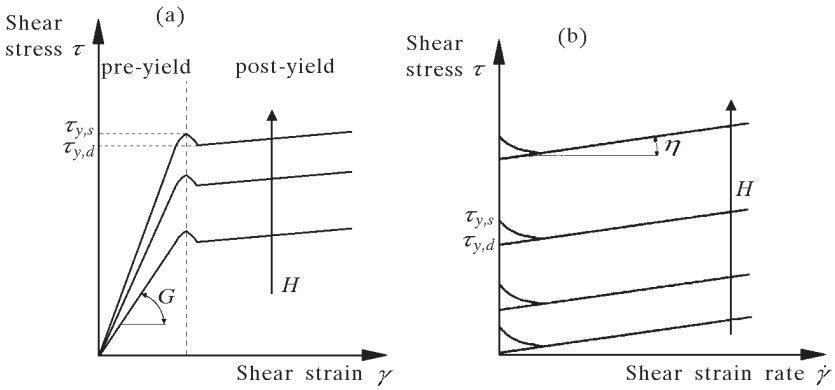

Fig. 3. (a) Shear stress-shear strain relationship of MR fluid; (b) observed post-yield shear behaviour of MR fluid

the MR fluid behaves like a viscoplastic material. Assuming that $\tau_{y,d} = \tau(H)$, the shear stress in the MR fluid is given by

$$\tau = \tau_y(H) + \eta\dot{\gamma} \qquad \tau \geqslant \tau_y(H) \tag{2.1}$$

where

η – viscosity

$\dot{\gamma}$ – shear strain rate.

However, in the post-yield area (for stress $\tau < 10^{-3}$ Pa (Jolly *et al.*, 2000)), the MR fluid behaves as a visco-elastic material and the fluid stress can be expressed as

$$\tau = G^*\gamma \qquad \tau < \tau_y(H) \tag{2.2}$$

where $G^* = G' + jG''$, is the complex shear modulus dependent on the magnetic field (Kormann *et al.*, 1994), in which G' means the storage modulus, and G'' – loss modulus. The storage modulus is proportionally related to the average energy required during one fluid deforming cycle in volume units, however, the loss modulus is proportional to the average energy stored during a cycle in fluid volume units. In reality, the MR fluid behaviour shows wide departures from Bingham's model, the most important of which is non-Newtonian behaviour for $H = 0$.

The research on MR fluid reactions sometimes shows that through jump-type changes in magnetic fields, the fluid stress changes have an asymptotically exponential character and gain 90% of their value in the time less than 10 ms. This means that MR fluids change their viscosity rapidly. It was stated in (Snyder *et al.*, 2000) that the changes in MR fluid properties from viscotic to

elastic follow a stress lower than 0.08% of the limited stress, which may limit the application of a MR fluid to adaptive structures, in which the stability is required in the pre-yield area.

3. Description of a MR damper

The construction of a MR linear damper is shown in Fig. 4a (longitudinal section) and Fig. 4b (cross section). The damper has a cylindrical shape and is filled with a MR fluid. The piston construction with an integrated coil ensures that the magnetic field is focused within a gap, inside a volume of the active portion of the MR fluid.

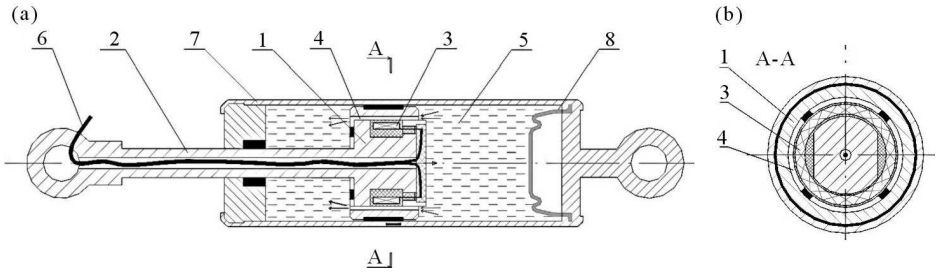

Fig. 4. (a) Longitudinal section: 1 – piston, 2 – rod, 3 – coil, 4 – gap, 5 – MR fluid, 6 – wires, 7 – housing, 8 – accumulator; (b) cross-section: 1 – piston, 3 – coil, 4 – gap

The damper operation is based on using the MR effect, which amounts to quick changes in the viscosity of the active portion of the fluid in the gap (Kordoński, 1993; Shulman and Kordoński, 1978). In the absence of a magnetic field ($I = 0 \Rightarrow H = 0$), the aggregates of magnetic particles are suspended in the carrier fluid (Fig. 2a), their magnetic moments are without any ordered structure and the resultant magnetic moment is equal to zero. In situations when external forces act on the piston, the damper resistance force depends, above all, on the fluid flow strain through the gap, resulting from the pressure differences between the cells from the fluid. Then the MR damper behaves like a viscotic damper. In the presence of an external field ($I \neq 0 \Rightarrow H \neq 0$), the aggregates are polarized and their magnetic moments are arranged along the field lines. These aggregates form chain-like structures parallel to the field lines (perpendicular to the fluid flow direction), thereby increasing the shear stress and the fluid viscosity and restricting its motion (Fig. 2b). The magnetic energy required to form such structures increases due

to the increase in the magnetic field. As a result, the fluid flow through the gap becomes limited, which draws increased hydraulic resistance for the piston movement and creates an additional damping force component, depending on the magnetic field (intensity of the current in the coil).

Due to the fact that the height of the gap in the damper is considerably less than its width and length (Fig. 4a and Fig. 4b) it can be seen that an adequate, accurate and comparative description of the mathematical fluid flow through the gap is a model with parallel plates (Spencer *et al.*, 1998). On this assumption, the input to the damping force consists of three parts: the force resulting from the static friction (depending on the type used in the damper seal), the force depending on the fluid viscosity, and the force depending on the magnetic field (more precisely, on the distribution of the magnetic flux density in the gap).

In order to control the MR damper, the pulse width modulation method (PWM) of the current in the coil is used. The PWM controller creates rectangular voltage signals of an amplitude A_m, and changeable co-factors $\alpha_w = T_i/T_p$, where T_i means the duration of the pulse, and T_p is set as the pulse repeat period (Fig. 5). If the damper coil is supplied by the voltage signal with this shape, the magnetic flux distribution is changed, which results in changes in the field line set-up in the damper magnetic circumference and related the damping force process.

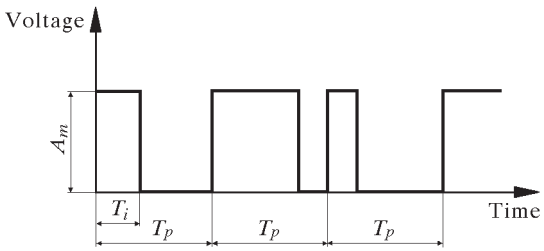

Fig. 5. Pulse width modulation

The theoretical evaluation of the magnetic flux density set up along the gap l and the magnetic field in the damper, in the case when the voltage on coil terminals is $U = 0\,\mathrm{V} \Rightarrow I = 0\,\mathrm{A}$ and $U = 3.0\,\mathrm{V} \Rightarrow I = 0.6\,\mathrm{A}$, are shown in Fig. 6 and Fig. 7, respectively (Sapiński *et al.*, 2001). The experimental process of the damping force for sinusoidal kinematic excitation of the damper piston (at the amplitude of $4 \cdot 10^{-3}\,\mathrm{m}$ and frequency 2.5 Hz) and the step voltage input, $U = 3.0\,\mathrm{V}$ ($I = 0.6\,\mathrm{A}$) and the connection time $t_1 = 0.488\,\mathrm{s}$, and disconnections time $t_2 = 0.992\,\mathrm{s}$ are shown in Fig. 8 (Sapiński *et al.*, 2001).

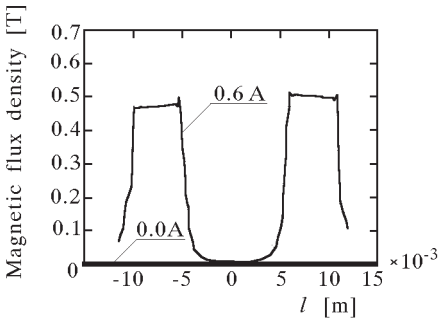

Fig. 6. Distribution of magnetic flux density along the gap for $I = 0.0\,\mathrm{A}$ and $I = 0.6\,\mathrm{A}$

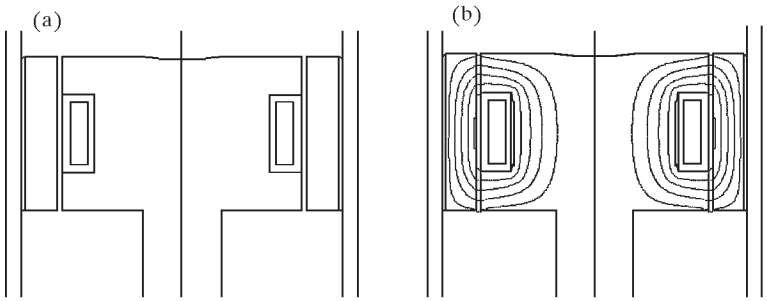

Fig. 7. Distribution of magnetic field lines: (a) $I = 0.0\,\mathrm{A}$, (b) $I = 0.6\,\mathrm{A}$

4. Parametric models of MR linear dampers

The parametric damper models are formulated using rheological structures, which, in various ways, approximate to the MR fluid behaviour, have direct influence on the accuracy of the damper behaviour prediction. Assuming, for example, that the MR fluid does not show hysteresis, it may be treated as a visco-plastic or visco-elastic material, which leads in the first case to the Bingham model, and in the second to the Bingham body, Gamota-Filisko and Li models. However, in view of the development in the MR fluids, the appearance of hysteresis leads to the Bouc-Wen or Spencer models. In order to analyse the above models, identification experiments were undertaken, the aim of which was to designate the parameter values for these models necessary for simulation (Sapiński, 2002).

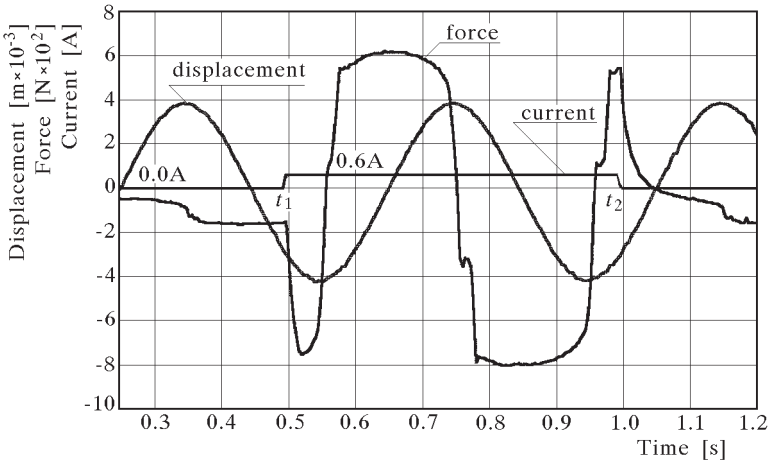

Fig. 8. Displacement vs. time; curent in the coil vs. time; damping force vs. time

4.1. Bingham model and Bingham body model

The idealisation of the visco-plastic MR damper model presented in Dyke *et al.* (1996) uses similarities in the rheological behaviour of ER and MR fluids and the similar techniques in the modelling of ER dampers (Sims *et al.*, 2000; Stanway *et al.*, 2000).

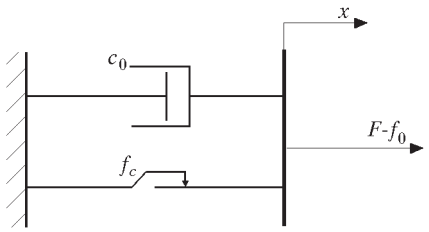

Fig. 9. Rheological structure of a MR damper for the Bingham model

In the rheological structure in Fig. 9, on which the Bingham model is based, there is a Coulomb friction element f_c placed parallel to the dashpot c_0. According to Bingham's MR damper model, for non-zero piston velocities $\dot{x}$, the damping force F can be expressed as

$$F = f_c \operatorname{sgn} \dot{x} + c_0 \dot{x} + f_0 \tag{4.1}$$

where f_c is the frictional force, c_0 is the viscous damping parameter, f_0 is the force due to the presence of the accumulator. This last simplification in the mo-

del results from the assumption that the elasticity replacing the accumulator activity has a low stiffness and linear characteristics.

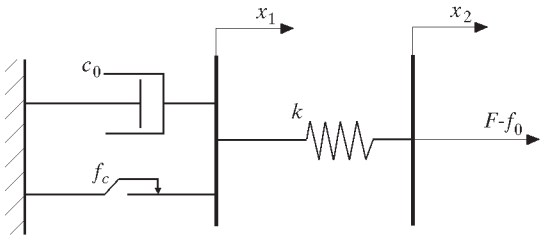

Fig. 10. Rheological structure of a MR damper for the Bingham body model

The Bingham body model, whose structure is presented in Fig. 10, differs from the Bingham model (Fig. 9) by the introducing of a spring k. Thus, the Bingham body model tries merging of three elements, that is, connecting in parallel the elements of St. Venant (plastic body model), Newton (Newton flow model) and the element of Hooke (elastic body model). This model, through its low shear stress, presents solid body behaviour, however only through a high shear stress, the liquid body. This occurs because, to a certain value of the applied force f_c (static friction force of the St. Venant element which refers to the shear stress $\tau_y(H)$ characteristic) only the spring will deform – similarly to the elastic Hooke body. If this force is greater than f_c the Bingham body will elongate (the body flows). The rate of the deformation will be proportional to the difference of the applied force and the friction force of the St. Venant element (i.e. $\dot{\gamma} \sim [\tau - \tau_y(H)]$).

According to the Bingham body model (see Fig. 10), the damping force F can be expressed as

$$F = \begin{cases} f_c \operatorname{sgn} \dot{x}_1 + c_0 \dot{x}_1 + f_0 & \text{for} \quad |F| > f_c \\ k(x_2 - x_1) + f_0 & \text{for} \quad |F| \leqslant f_c \end{cases} \tag{4.2}$$

where the parameters f_c, c_0, f_0 have the same meaning as in equation (4.1) and k represents the stiffness of the elastic body (Hooke model).

4.2. Gamota-Filisko model

An extension of the Bingham MR damper model is the visco-elasto-plastic model formulated by Gamota and Filisko (Dyke *et al.*, 1996). This extension depends on connection of the Bingham, Kelvin-Voight body and Hooke body models (Fig. 11). The Kelvin-Voight model represents a solid body, whose maximum elongation exclusively depends on the applied force (independent of time).

Characteristic for this model is the appearance of the creeping phenomenon (elongation gradually increases as a result of delayed damper activity). Hooke's model, in turn, for which the spring elongation is proportional to the applied force and independent of time, represents the ideal elastic body.

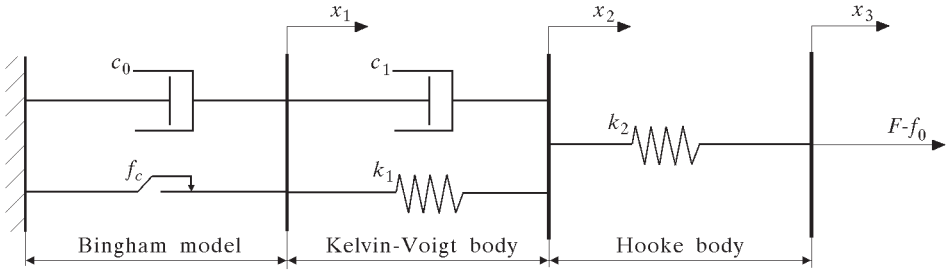

Fig. 11. Rheological structure of a MR damper for the Gamota-Filisko model

The damping force in the Gamota-Filisko model (see Fig. 11) can be described as

$$F = \begin{cases} k_1(x_2 - x_1) + c_1(\dot{x}_2 - \dot{x}_1) + f_0 = \\ c_0\dot{x}_1 + f_c \operatorname{sgn}\dot{x}_1 + f_0 = k_2(x_3 - x_2) + f_0 & \text{for} \quad |F| > f_c \\ k_1(x_2 - x_1) + c_1\dot{x}_2 + f_0 = k_2(x_3 - x_2) + f_0 & \text{for} \quad |F| \leqslant f_c \end{cases} \tag{4.3}$$

where

- c_0, f_0, f_c – parameters representing the viscous damping, force due to the presence of the accumulator, frictional force (Bingham model)
- k_1, c_1 – parameters representing the stiffness and damping of the body (Kelvin-Voigt model)
- k_2 – parameter representing the stiffness of the elastic body (Hooke model).

It should be noted that when $|F| \leqslant f_c$, then $\dot{x}_1 = 0$, which means that when the friction force f_c related with the new stress in the fluid is greater than the damping force F, the piston remains motionless.

4.3. Li model

Another view of visco-elasto-plastic properties of MR fluids in the modelling of MR damper behaviour is the model composed by Li (Li *et al.*, 2000). This model is divided into two areas; pre- and post-yield. In these areas the MR fluid shows visco-elastic and visco-plastic body properties, respectively, which conform to the rheological structures presented in Fig. 12.

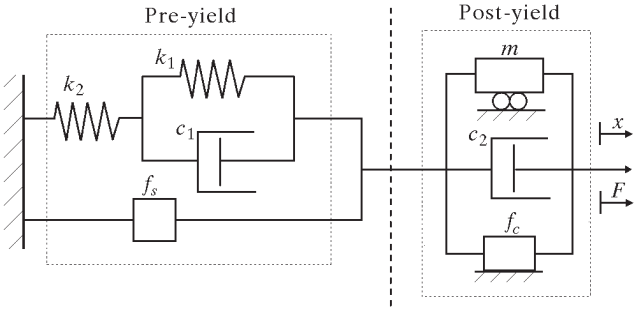

Fig. 12. Rheological structure of a MR damper for the Li model

Li proposed a description of a MR fluid state in the pre-yield area of a visco-elastic model, in which Hooke's body (spring k_2) was joined with Kelvin-Voight's body (spring k_1 and dashpot c_1). Besides the visco-elastic force f_{ve}, a contribution to the damping force F in the pre-yield area also carries the static friction force f_s, resulting from the applied type of seal in the damper. Accordingly, the damping force F in the pre-yield area can be written as

$$F = f_{ve} + f_s \tag{4.4}$$

where the force f_{ve} is described by the equation

$$\dot{f}_{ve} + \frac{k_1 + k_2}{c_1} f_{ve} = \frac{k_1 \cdot k_2}{c_1} x + k_2 \dot{x} \tag{4.5}$$

where the damping force F crosses the plastic flow force f_c (when $\tau \geqslant \tau_y(H)$), the damper operates in the post-yield area. Then damping force is also equal to the visco-plastic force, to which, besides the friction force connected with the fluid shear stress f_c, the viscotic force and inertial force contribute, which can be written as

$$F = f_c \operatorname{sgn} \dot{x} + c_2 \dot{x} + m\ddot{x} \tag{4.6}$$

where c_2 is a co-factor of viscotic friction, and m is the mass of replaced MR fluid dependent on the amplitude and frequency of a kinematic excitation applied to the piston. As such, the damping force in the Li model is expressed as: equation (4.4) in the pre-yield area ($|F| \leqslant f_c$) and equation (4.6) in the post-yield area ($|F| > f_c$).

4.4. Bouc-Wen model

In structures showing hysteresis, through dynamic pressure (especially when the considered structure has a non-elastic character), the restoring force depends not only on the moment of the displacement, but also on the

past events of the structure. This fact creates certain problems in the modelling of structures with hysteresis creating vibration situations. To solve this problem, various approximation methods are applied (Brokate and Sprekels, 1996), which lead to various models allowing the consideration of the hysteresis in the MR and ER damper behaviour. McClamroch and Gavin (1995) and Hsu and Meyer (1995) used trigonometric functions to describe the hysteresis.

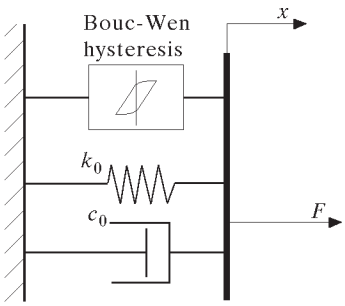

Fig. 13. Rheological structure of a MR damper for the Bouc-Wen model

This approach, however, does not allow the consideration of the damping force saturation which occurs in periods of high piston velocity. In turn, Werely *et al.* (1998) presented a biviscotic model with hysteresis, Sims *et al.* (2000) modified Bingham's plastic model (Dyke *et al.*, 1996), and the Choi (Choi *et al.*, 2001) model, in which the dependence of the damping force on the velocity is a 6th order polynomial with respect to the piston velocity of the damper. A further development of the MR damper model, considering the appearance of the hysteresis and damping force saturation, is the Bouc-Wen model (Dyke *et al.*, 1996), whose rheological structure is presented in Fig. 13. In this model the hysteresis approximation method proposed by Wen (1976) is applied. Accordingly, in structures showing hysteresis, the restoring force $Q(x, \dot{x})$ is the sum of two components, without the hysteresis $g(x, \dot{x})$ and with $h(x)$

$$Q(x, \dot{x}) = g(x, \dot{x}) + h(x) + ... \tag{4.7}$$

The component $h(x)$ is defined by an equation, which refers to the displacement x and z (evolutional variable), through which the position of the equation is dependent on whether n is an even or odd number. For an odd n, the equation is

$$\dot{z} = -a|\dot{x}|z^n - \beta\dot{x}|z^n| + A\dot{x} \tag{4.8}$$

however for an even number

$$\dot{z} = -a|\dot{x}|z^{n-1} - \beta\dot{x}z^n + A\dot{x} \tag{4.9}$$

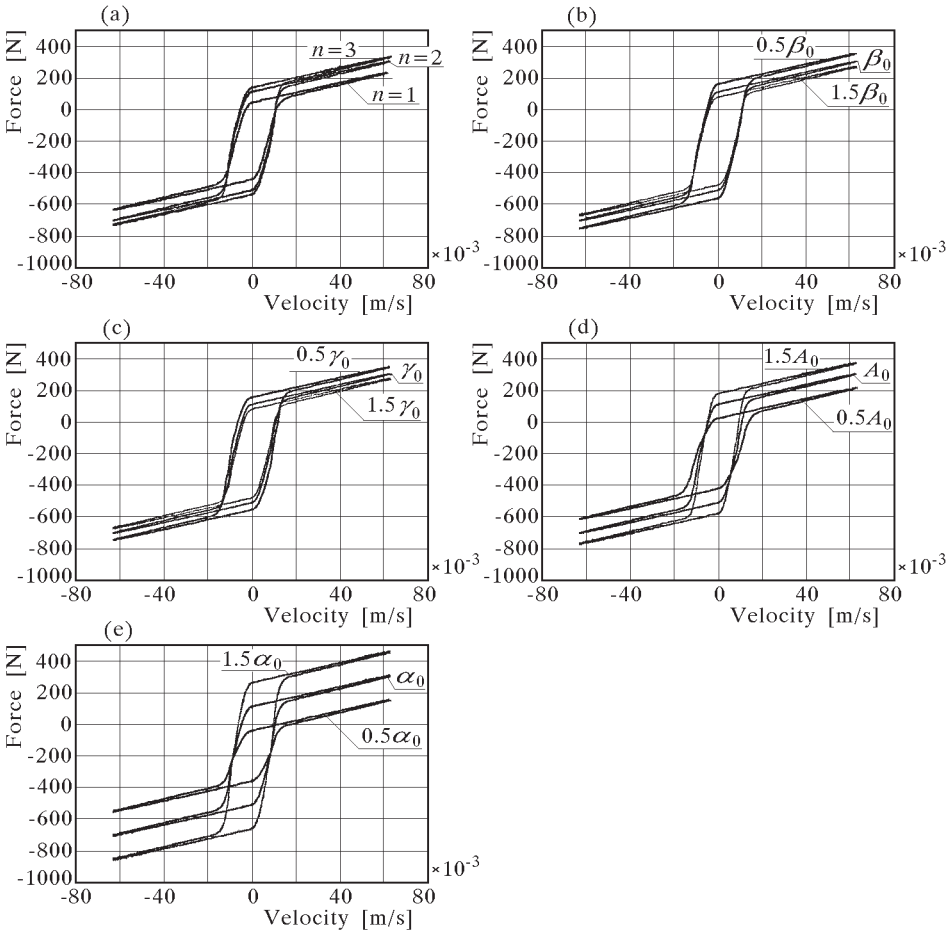

Fig. 14. Influence of parameters: n, β, γ, A, α on force-velocity curves

The influence of n on the dependence of the MR damper force on the velocity, through the chosen parameters of the Bouc-Wen model and for $n = 1$, $n = 2$, $n = 3$, is shown in Fig. 14a. In Wen (1976) it is stated that using this method, the prediction accuracy of behavioural structures with hysteresis is satisfactory as compared with the experimental results gained for $n = 2$.

The damping force in the Bouc-Wen model can be written as

$$F = c_0\dot{x} + k_0(x - x_0) + \alpha z \tag{4.10}$$

where the evolutional variable z is described by the equation

$$\dot{z} = -\gamma|\dot{x}|z|z|^{n-1} - \beta\dot{x}|z|^n + A\dot{x} \tag{4.11}$$

where

- β, γ, A – parameters representing the control of the linearity during unloading and the smoothness of the transition from the pre-yield to post-yield area
- α – parameter representing the stiffness for the damping force component associated with the evolution variable z
- k_0 – parameter representing the stiffness of the spring associated with the nominal damper due to the accumulator
- c_0 – parameter representing viscous damping
- c_1 – parameter representing the dashpot included in the model to produce the roll-off at low velocities
- x_0 – parameter representing the initial displacement of the spring with the stiffness k_0.

The influence of the parameters β, γ, A, α on the accuracy of hysteresis prediction in the damping force-velocity curve is shown for the Bouc-Wen model in Fig. 14b,c,d,e.

4.5. Spencer model

The extension of the Bouc-Wen model proposed by Spencer concerns the introduction of an additional dashpot c_1 and spring k_1. This suits the rheological structure shown in Fig. 15.

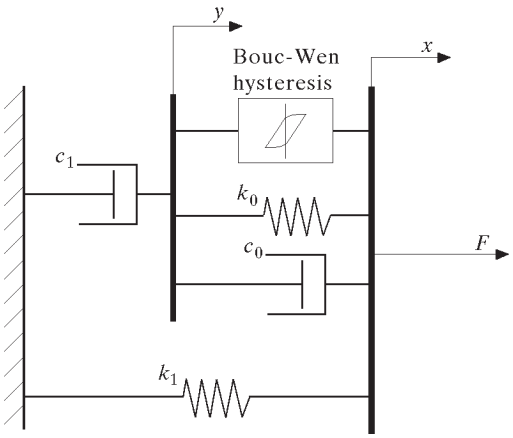

Fig. 15. Rheological structure of a MR damper for the Spencer model

Damping force in Spencer's model can be expressed as

$$F = az + c_0(\dot{x} - \dot{y}) + k_0(x - y) + k_1(x - x_0) \tag{4.12}$$

or can be also written as

$$F = c_1\dot{y} + k_1(x - x_0) \tag{4.13}$$

where the displacements z and y are respectively defined as

$$\begin{aligned} \dot{z} &= -\gamma|\dot{x} - \dot{y}|z|z|^{n-1} - \beta(\dot{x} - \dot{y})|z|^n + A(\dot{x} - \dot{y}) \\ \dot{y} &= \frac{1}{c_0 + c_1}[az + c_0\dot{x} + k_0(x - y)] \end{aligned} \tag{4.14}$$

The parameter c_1 suits viscotic damping at higher velocities, the parameter k_1 corresponds to the stiffness representing the accumulator, the parameter k_0 stands for the stiffness at higher velocities, however, the remaining parameters in equations (4.12)-(4.14) have the same meaning as in the Bouc-Wen model.

5. Identification experiment

In order to simulate the damper behaviour through the use of the described models it is necessary to define the values of their parameters. For this purpose, experimental tests were carried out on the MR damper of RD-1005 type, produced by Lord Corporation. The scheme of the experimental setup for the damper tests is shown in Fig. 16.

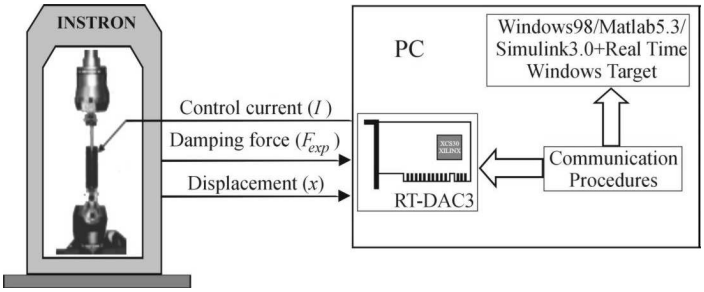

Fig. 16. Scheme of the experimental setup for examinations of a MR linear damper

The tests were conducted at the experimental setup, see Fig. 16, with a computer-controlled INSTRON test machine, data acquisition system with the multi I/O board of RT-DAC3 type and in the software environment of Matlab/Simulink, and Real Time Workshop Target. The machine was programmed to move up and down in a sinusoidal wave for seven levels of the

frequency f (0.5, 1, 2.5, 4, 6, 8, 10) Hz. The responses were measured for eight levels of the control current I (0.0, 0.2, 0.4, 0.6, 0.8, 1.0, 1.2, 1.6) A. The way of conducting the tests and the parameter identification methods for the Bingham and Spencer models is carefully described by Sapiński (2002). Due to the requirements of this work, the identification was extended to the Bingham body, Gamota-Filisko, Li and Bouc-Wen models.

For the parameter computation the following criteria have been adopted (Spencer *et al.*, 1998)

$$\varepsilon_t = \int_0^T (F_e - F_m)^2 \, dt \qquad \varepsilon_x = \int_0^T (F_e - F_m)^2 \Big| \frac{dx}{dt} \Big| \, dt$$
$$\varepsilon_{\dot{x}} = \int_0^T (F_e - F_m)^2 \Big| \frac{d\dot{x}}{dt} \Big| \, dt \tag{5.1}$$

where F_e and F_m denote the damping force derived from the experiments and models, respectively. The criteria define for each model the difference between F_e and F_m as a function of time $(5.1)_1$, displacement $(5.1)_2$ and velocity $(5.1)_3$. For computation the CONSTR subroutine available in Matlab optimisation toolbox was used. The procedure finds the local minimum of the function of several variables under some constrains imposed on the variables. The parametric values of the models obtained by this procedure are presented in Table 2 - 7.

Table 2. Parameters of Bingham model

Current	Value of the parameter		
I [A]	f_c [N]	c_0 [Ns/m]	f_0 [N]
0.0	43.95	735.90	195.51
0.4	262.13	3948.70	186.28

Table 3. Parameters of Bingham body model

Current	Value of the parameter			
I [A]	f_c [N]	c_0 [Ns/m]	f_0 [N]	k [N/m]
0.0	43.95	735.90	195.51	895.00
0.4	262.13	3948.70	186.28	3623.00

Table 4. Parameters of Gamota-Filisko model

Current	Value of the parameter					
I [A]	f_c [N]	c_0 [Ns/m]	c_1 [Ns/m]	k_1 [N/m]	k_2 [N/m]	f_s [N]
0.0	43.95	735.90	2026.00	1387.00	895.00	195.51
0.4	262.13	3948.70	16487.00	8421.00	3623.00	186.28

Table 5. Parameters of Li model

Current	Value of the parameter			
I [A]	f_c [N]	f_s [N]	c_1 [Ns/m]	c_2 [Ns/m]
0.0	43.95	195.51	4983.00	12120.00
0.4	262.13	186.28	9987.00	6103.00

Current	Value of the parameter		
I [A]	k_1 [N/m]	k_2 [N/m]	m [kg]
0.0	998.10	10053.00	0.07
0.4	998.10	61432.00	0.07

Table 6. Parameters of Bouc-Wen model

Current	Value of the parameter			
I [A]	α [N/m]	c_0 [Ns/m]	A [-]	β [m^{-1}]
0.0	7507.50	549.86	125.18	1097222.00
0.4	38988.04	3195.43	215.20	1880301.00

Current	Value of the parameter		
I [A]	γ [m^{-1}]	k_0 [N/m]	x_0 [kg]
0.0	1340385.00	1610.14	0.13
0.4	1696138.00	2169.09	0.92

Table 7. Parameters of Spencer model

Current	Value of the parameter				
I [A]	α [N/m]	c_0 [Ns/m]	c_1 [Ns/m]	k_0 [N/m]	A [-]
0.0	24830.30	553.90	38519.90	1037.4	25.70
0.4	86665.00	1965.10	20626.50	2807.8	29.37

Current	Value of the parameter			
I [A]	β [m^{-1}]	γ [m^{-1}]	k_1 [N/m]	x_0 [kg]
0.0	1387320.0	3862730.00	651.50	0.30
0.4	1198420.0	52260.00	675.30	0.27

6. Simulation of behaviour of a MR linear damper

Based on the resulting parameters, the theoretical relationships were established for: damping force vs. time, damping force vs. displacement and damping force vs. velocity, using Matlab/Simulink. As an example, these curves compared with the experimental data for $f = 2.5\,\mathrm{Hz}$; $I = 0\,\mathrm{A}$ and $I = 0.4\,\mathrm{A}$ are shown in Fig. 17, Fig. 18 and Fog. 19, respectively. The lines (▬ ▬) indicate the experimental data, while the theoretical curves are marked with (▬▬).

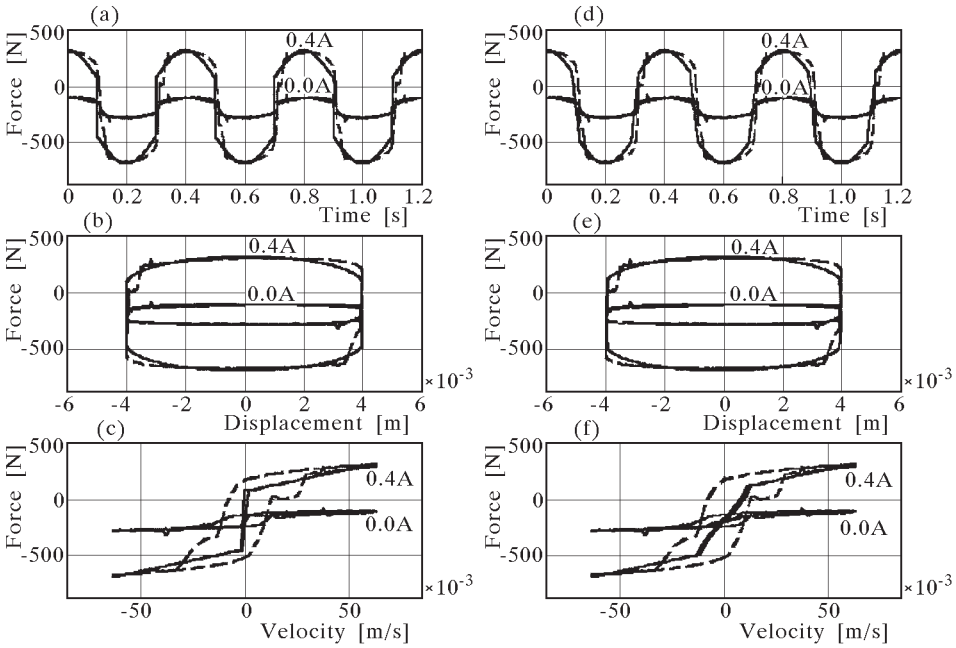

Fig. 17. Comparison of force-time, force-displacement and force-velocity curves between measurement (▬ ▬) and prediction (▬▬) for the Bingham model: (a), (b), (c), for the Bingham body model: (d), (e), (f)

Analysis of the results gained from the simulations and their comparison with the experimental data allows us to estimate the accuracy with which we can predict the actual MR damper behaviour using the considered models with regard to various MR fluid properties (visco-plastic, visco-elasto-plastic, and visco-elastic with hysteresis).

The quality of the visco-plastic Bingham model is its simplicity, however its shortcoming is that for zero piston velocity the damping force does not

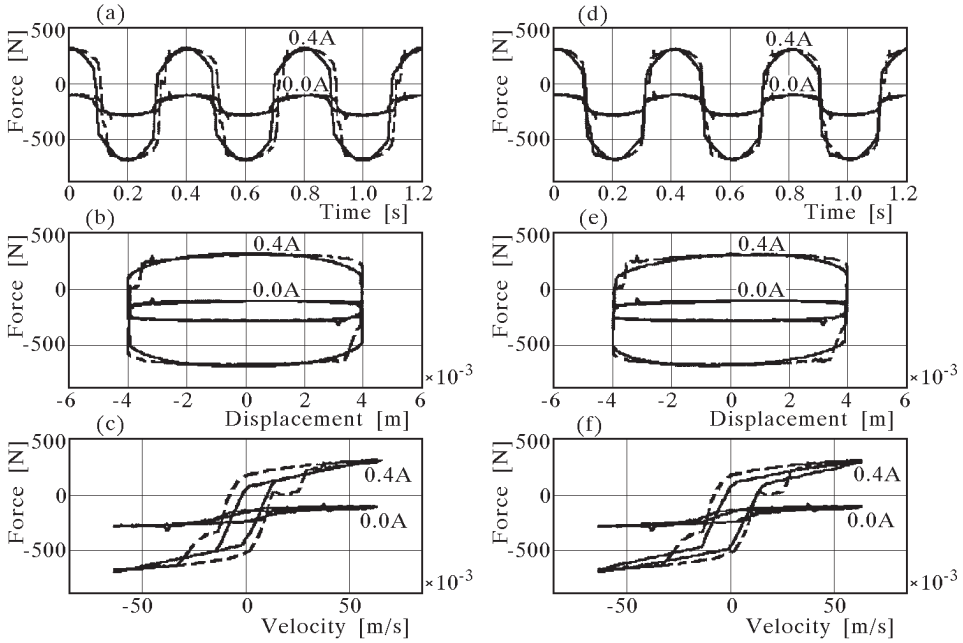

Fig. 18. Comparison of force-time, force-displacement and force-velocity curves between measurement (– – –) and prediction (———) for the Gamota-Filisko model: (a), (b), (c), for the Li model: (d), (e), (f)

equal zero, and that the force in the friction element is equal to the applied force. The force-velocity curve, which can be predicted with the use of this model, is one-to-one, but does not suit the experimental data (that is not one-to-one). At the velocity equal to zero, the measured force and acceleration have opposite signs: the additional damping force – negative acceleration (additional displacement) and vice-versa.

As a result of the spring employed in the Bingham model, the MR damper parametric model representing the visco-elasto-plastic model of the Bingham body was obtained. The effect of this spring is the proportional change of the damping force with velocity.

The Gamota-Filisko model allows us to predict the force-velocity curve which more closely relates to the experimental data than in the Bingham body model. The characteristic feature of this model is that if the velocity approaches zero, the decrease in the damping c_1, may generate the roll-off observed in the force-velocity curve (Dyke *et al.*, 1996).

The advantage of the visco-elasto-plastic model proposed by Li lies in the possibility of more accurate capturing of MR damper dynamic properties than

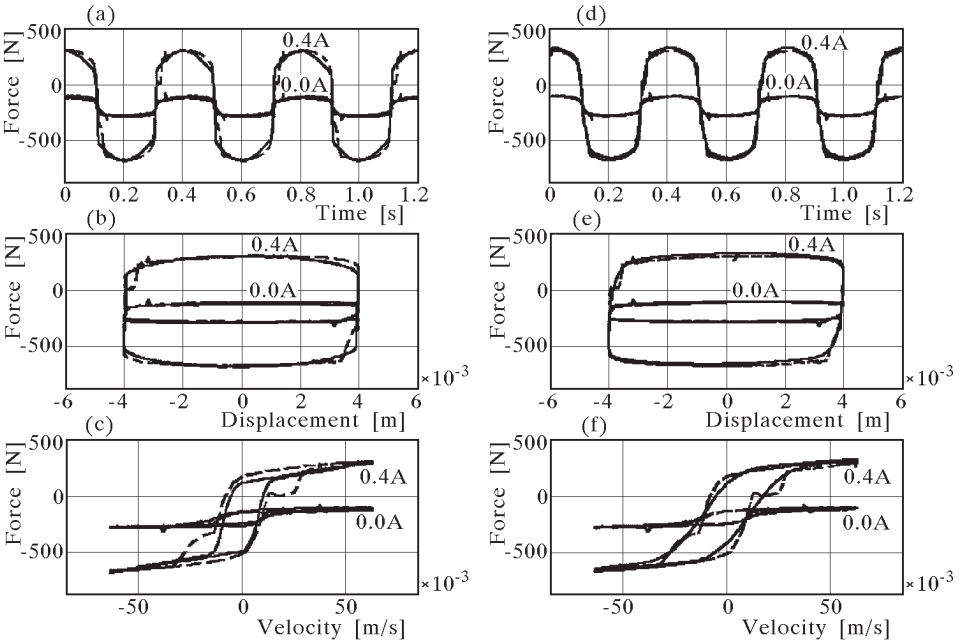

Fig. 19. Comparison of force-time, force-displacement and force-velocity curves between measurement (– – –) and prediction (———) for the Bouc-Wen model: (a), (b), (c), for the Spencer model: (d), (e), (f)

in the Gamota-Filisko model. That is due to distinguishing pre- and post-yield areas of the MR fluid operating range. In addition, this model enables us to investigate the influence of the MR fluid inertia on the damping force (Li *et al.*, 2000).

The force-displacement curves predicted by the Bouc-Wen model are accurate in comparison to the experimental data (more accurate than in the visco-elasto-plastic models described above). However, at low velocities (similarly to the Bingham model) there appears a nonlinear character of the force-velocity curves, and therefore, it does not apply to the area in which the accelaration and the velocity have different signs.

The visco-elastic model with the hysteresis formulated by Spencer enables us to the most accurately predicted actual MR damper behaviour (from the discussed models) in the whole operating range, also in the area of low velocities in which the acceleration and the velocity have different signs. It refers to all curves, i.e. force-time, force-displacement and force-velocity ones.

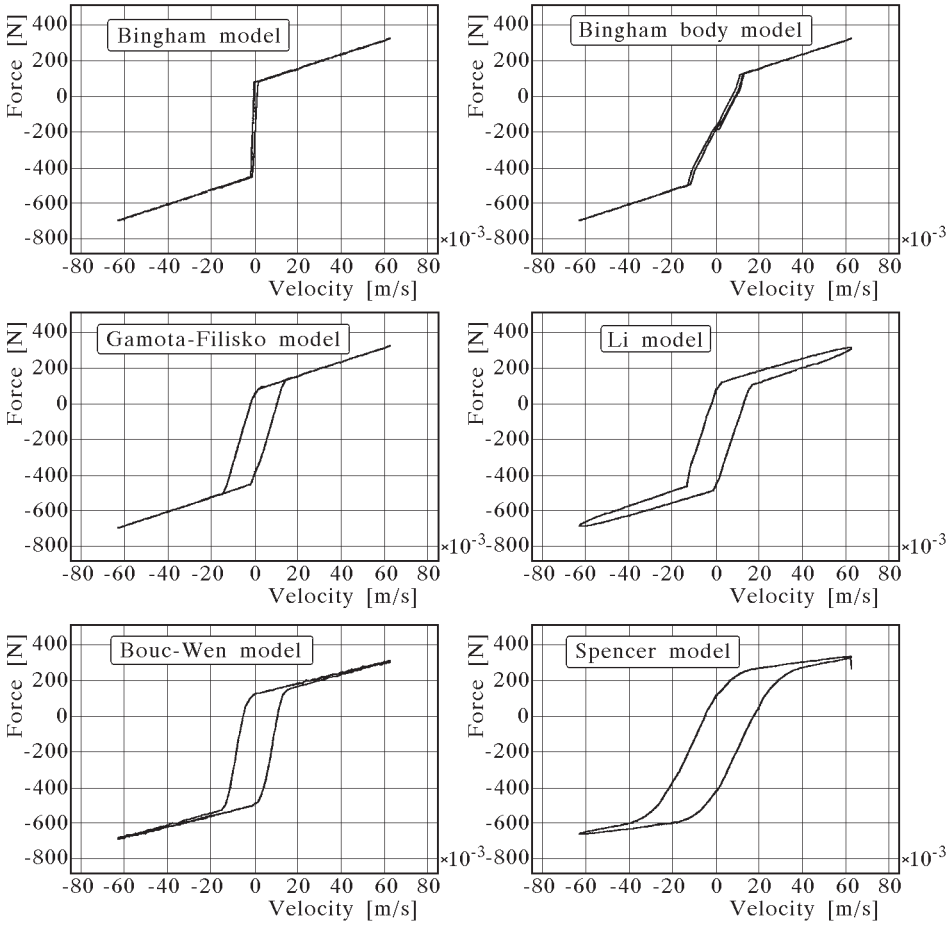

Fig. 17. Comparison of predicted force-velocity curves for considered MR damper models: $f = 2.5\,\mathrm{Hz}$, $I = 0.4\,\mathrm{A}$

7. Summary

In this paper, analysis of parametric models of MR linear dampers has been undertaken. The analysis has been concerned with various behaviour characteristics of a MR fluid, which fills the damper, i.e. visco-plastic, visco-elasto-plastic and visco-elastic with a histeresis. Based on the identification experiment, the parameters for these models were designated for a sinusoidal kinematic excitation and constant control current. The analysis showed that basic difficulties in formulation of the models, which could effectively portray

the actual behaviour of the MR damper were caused by the hysteresis and a jump-type phenomenon resulting from the specific properties of the MR fluid. This is illustrated in Fig. 20, in which the force-velocity curves computed for each considered model are presented.

It can be clearly seen that if the rheological structure representing the fluid behaviour in the model is too simple, then the predicted curves (force vs. time, force vs. displacement and force vs. velocity) becomes less accurate. The consequence of this is limitation of the applied models, an example of which may be Bingham's model, which captures damper features well, but inaccurately represents its behaviour for near-zero piston velocity. This means that Bingham's model is not useful in control problems. The key factor is to take into account the magnetic field saturation, which is an inherent MR damper feature.

There are also difficulties in finding the solution to some equations of the analysed models. This concerns, in particular, extended models taking into account the appearance of a hysteresis (Bouc-Wen and Spencer), which are difficult to solve analytically. Similarly, the Gamota-Filisko and Li models are difficult to solve numerically (numerical integration reguires a time step of 10^{-6} s). As experience shows, the stiff character of differential equations in the Gamota-Filisko and Li models entails that they can not be used as governing formulas for real-time controllers.

Which of the analysed models will be useful for the control problems will be decided by the future research aiming at the obtaining of the actual relationship between the model parameters and the control signal.

Acknowledgement

The research work has been supported by the State Committee for Scientific Research as a part of grant No. 8T07B 03520

References

1. Bolter R., Janocha H., 1997, Design rules for MR actuators in different working modes, *Proc. of SPIE*, **3045**, 148-159
2. Brokate M., Sprekels J., 1996, *Hysteresis and Phase Transitions*, Applied Mathematical Sciences, SpringerVerlag, 121
3. Carlson J.D., Spronston J.L., 2000, Controllable fluids in 2000 status of ER and MR fluid technology, *"Actuator 2000" – 7th International Conference on New Actuators*

4. CHOI S.B., LEE S. K., PARK Y.P., 2001, A hysteresis model for the field – dependent damping force of a magnetorheological damper, *Journal of Sound and Vibration*, **245**, 375-383

5. DYKE S., SPENCER B., SAIN M., CARLSON J., 1996, Phenomenological model of a magnetorheological damper, *Journal of Engineering Mechanics*

6. GANDHI F., CHOPRA I., 1996, A time-domain non-linear viscoelastic damper model, *Smart Materials and Structures*, **5**, 517-528

7. GINDER J.M., 1996, Rheology controlled by magnetic fields, *Encyclopedia of Applied Physics*, **16**, 487-503

8. HSU J.C., MEYER A.U., 1995, Modern Control Principles and Applications, McGraw-Hill, 116-120

9. JOLLY M., BENDER J.W., CARLSON J.D., 1999, Properties and applications of commercial magnetorheological fluids, *Journal of Intelligent Material Systems and Structures*, **10**, 5-13

10. KAMATH G.M., WERELY N.M., 1997, Nonlinear viscoelastic-plastic mechanisms based model of an electrorheological damper, *Journal of Guidance, Control and Dynamics*, **6**, 1125-1132

11. KEMBŁOWSKI Z., 1973, *Reometria płynów nienewtonowskich*, WNT, Warszawa

12. KORDOŃSKI W., 1993, Elements and devices based on magnetorheological effect, *Journal of Intelligent Systems and Structures*, **4**, 65-69

13. KORMANN C., LAUN M., KLETT G., Actuator 94, *4th Int. Conf. On New Actuators*, eds. H. Borgmann and Lenz, Axon Technologies Consult GmbH, 271

14. LI W.H., YAO G.Z., CHEN G., YEO S.H., YAP F.F., 2000, Testing and steady state modelling of a linear MR damper under sinusoidal loading, *Smart Materials and Structures*, **9**, 95-102

15. MCCLAMROCH N.H., GAVIN H.P., 1995, Closed loop structural control using electrorheological dampers, *Proceedings of American Control Conferences*, Seattle, Washington

16. SAPIŃSKI B., KRUPA S., JARACZEWSKI M., Influence of magnetic field distribution of linear magnetorheological damper, *25th International Conference on Fundametals of Electrotechnics and Circuit Theory, IC-SPETO*, May 22-25, 2002, Gliwice-Ustroń 2001, Poland, 29-32

17. SAPIŃSKI B., 2002, Parametric identification of MR linear automotive size damper, *Journal of Theoretical and Applied Mechanics*, **40**, 703-722

18. SAPIŃSKI B., 2002, Non-parametric representations of MR linear damper behavior, *IUTAM Symposium on Dynamics of Advanced Materials and Smart Structures*, Yonezawa, Japan, Kluwer Academic Publishers, 347-357

19. Shulman Z.P., Kordoński V.I., 1978, *The Magnetorheological Effect*, Science and Technic, Mińsk

20. Shulman Z.P., Kordoński V.I., Zaltsgendler E.A., Prokhorov I.V., Khusid B.M., Demchuk S.A., 1985, *Structure, Physics and Dynamic Properties of MRs*, Bielarus

21. Sims N.D., Peel D.J., Stanway R., Johnson A.R., Bulough W.A., 2000, The electrorheological long-stroke damper: a new modeling technique with experimental validation, *Journal of Sound and Vibration*, **229**, 207

22. Snyder R.A., Kamth G.M., Werely N.M., 2000, Characterization and analysis of magnetorheological damper behaviour due to sinusoidal loading, *Proceedings of SPIE Symposium on Smart Materials and Structures*, **3989**, New Port Beach, California, 213-229

23. Spencer B.F. Jr., Yang G., Carlson J.D., Sain M.K., 1998, Smart dampers for seismic protection of structures: a full-scale study, *Proc. 2 nd World Conference on Structural Control*

24. Stanway R., Sims N.D., Johnson A.R., 2000, Modelling and control of a magnetorheological vibration isolator, *Smart Structures and Materials 2000: Damping and Isolation, Proc. of SPIE*, **3989**, 184-192

25. Sunakoda K., Sodeyama H., Iwata N., Fujitani H., Soda S., 2000, Dynamic characteristics of magnetorheological fluid damper, *Smart Structures and Materials: Damping and Isolation, Proc. of SPIE*, **3989**, 194-202

26. Weiss K.D., Carlson J.D., Nixon D.A., 1994, Viscoelastic properties of magneto-electro-rheological fluids, *Journal of Intelligent Systems and Structures*, **5**, 772

27. Wen Y., 1976, Method for random vibration of hysteretic systems, *Journal of the Engineering Mechanics Division*, 249-263

28. Wereley N.M., Pang L., Kamath G.M., 1998, Idealized hysteresis modeling of electrorheological and magnetorheological dampers, *Journal of Intelligent Material Systems and Structures*, **9**, 642

Analiza modeli parametrycznych liniowego tłumika magnetoreologicznego

Streszczenie

W pracy dokonano analizy parametrycznych modeli fenomenologicznych liniowego tłumika magnetoreologicznego (MR), które odpowiadają różnym strukturom reologicznym cieczy MR wypełniającej tłumik. Przedstawiono własności cieczy, budowę

tłumika oraz modele parametryczne tłumika przybliżające w rożny sposób rzeczywiste zachowanie cieczy MR. W oparciu o symulacje komputerowe pokazano efektywność modeli do przewidywania rzeczywistego zachowanie liniowego tłumika MR. Wartości parametrów modeli wykorzystywane w symulacjach wyznaczono na podstawie eksperymentu identyfikacyjnego.

Manuscript received October 1, 2002; accepted for print January 14, 2003